2012

Short-Range Correlations and Cooling of Ultracold Fermions in the Honeycomb Lattice

Baoming Tang, *Georgetown University*
Thereza Paiva, *Universidade Federal do Rio de Janeiro*
Ehsan Khatami, *Georgetown University*
Marcos Rigol, *The Pennsylvania State University*

Short-Range Correlations and Cooling of Ultracold Fermions in the Honeycomb Lattice

Baoming Tang,[1,2] Thereza Paiva,[3] Ehsan Khatami,[1,2] and Marcos Rigol[1,2]

[1]*Department of Physics, Georgetown University, Washington, DC 20057, USA*

[2]*Physics Department, The Pennsylvania State University, 104 Davey Laboratory, University Park, Pennsylvania 16802, USA*

[3]*Instituto de Fisica, Universidade Federal do Rio de Janeiro Cx.P. 68.528, 21941-972 Rio de Janeiro RJ, Brazil*

(Received 31 May 2012; published 12 November 2012)

We use determinantal quantum Monte Carlo simulations and numerical linked-cluster expansions to study thermodynamic properties and short-range spin correlations of fermions in the honeycomb lattice. We find that, at half filling and finite temperatures, nearest-neighbor spin correlations can be stronger in this lattice than in the square lattice, even in regimes where the ground state in the former is a semimetal or a spin liquid. The honeycomb lattice also exhibits a more pronounced anomalous region in the double occupancy that leads to stronger adiabatic cooling than in the square lattice. We discuss the implications of these findings for optical lattice experiments.

DOI: 10.1103/PhysRevLett.109.205301 PACS numbers: 67.85.−d, 05.30.Fk, 37.10.Jk, 71.10.Fd

In recent years, the isolation of graphene flakes [1] has generated a revolution in solid state physics [2]. Graphene is an atom thick structure with carbon atoms arranged in a honeycomb lattice geometry, which features low energy excitations that are massless Dirac fermions. Given its reduced coordination number, graphene has also opened a new venue to create exotic quantum phases. Based on quantum Monte Carlo (QMC) simulations of the half filled one-band Hubbard model, Meng *et al.* [3] have argued that a spin-liquid ground state may be realized in this lattice geometry at intermediate interaction strengths. Earlier works had found the ground state to be a semimetal in the weakly-interacting regime and a Mott insulator with long-range antiferromagnetic (AF) correlations in the strongly-interacting regime [4,5]. The finding of an intermediate spin-liquid phase, recently challenged by another QMC study that considered larger lattice sizes [6], motivated much theoretical work in related models [7–15].

Experiments on fully tunable artificial graphene-like lattices now offer a pathway to study the physics above, and more, in a controlled way [16–19]. Motivated by those experimental advances, especially by the availability of an ultracold lattice fermion setup [18], where on-site interactions, hopping amplitudes, doping, and temperature can be fully controlled using Feshbach resonances, changing the lattice depth and the number of fermions in the gas, and varying the cooling time [20], respectively, we study thermodynamic properties and short-range correlations of two-component correlated fermions in the honeycomb lattice.

We show that such a system exhibits several unexpected properties when compared with its square lattice counterpart. For example, at a finite temperature, it may be less compressible in the weakly-interacting regime where its ground state is a semimetal, while the latter becomes less compressible in the presence of strong interactions when both lattices have an insulating ground state. We also identify temperature regimes in which, surprisingly, (i) nearest-neighbor (NN) spin correlations are stronger and (ii) a more significant anomalous region can be seen in the derivative of the double occupancy with respect to temperature, in the honeycomb lattice than in the square lattice.

We consider the one-band Hubbard Hamiltonian

$$\hat{H} = -t \sum_{\langle i,j \rangle \sigma} (\hat{c}^{\dagger}_{i\sigma} \hat{c}_{j\sigma} + \text{H.c.}) + U \sum_{i} \hat{n}_{i\uparrow} \hat{n}_{i\downarrow}, \qquad (1)$$

where standard notation has been used [21]. At half filling, in the square lattice, the ground state of this model is an AF Mott insulator for any $U > 0$ [21], while, in the honeycomb lattice, it has been recently argued to be a semimetal for $0 \leq U/t \lesssim 3.5$, an AF Mott insulator for $U/t \gtrsim 4.3$, and a gapped spin liquid in between [3].

In this Letter, to study the properties of the Hamiltonian [Eq. (1)] in the honeycomb and square lattices, we utilize two unbiased computational approaches, the determinantal quantum Monte Carlo (DQMC) technique [22–24] and numerical linked-cluster expansions (NLCEs) [25–27]. DQMC simulations are performed in finite-size systems (with 100 and 96 sites for the square and honeycomb lattices, respectively) using a small discretized imaginary time ($\Delta\tau \times t = 0.05$). NLCE calculations, on the other hand, provide exact results in the thermodynamic limit but converge down to a temperature that is determined by the divergence of correlations and the largest cluster sizes that we can consider. Here, we include clusters up to the ninth order in the site expansion and use Wynn and Euler resummation algorithms to extend the region of convergence to lower temperatures [25,26,28]. DQMC calculations and NLCEs are complementary as the former provides more accurate results down to lower T for $U \lesssim w$, where w is the noninteracting bandwidth ($w = 6t$ for the honeycomb lattice and $w = 8t$ for the square lattice) while the latter is better suited for $U > w$ [29]. In the region where DQMC statistical errors are small and

NLCEs converge, we obtain an excellent agreement between both approaches.

In optical lattice experiments, single site addressability [30,31] makes possible an accurate determination of the equation of state [density (n) vs chemical potential (μ)] of lattice Hamiltonians of interest. This equation of state determines the shape of the experimental density profiles and, when obtained at low enough temperatures, allows one to identify the presence of a single particle gap in the spectrum. In the inset of Fig. 1(a), we show the equation of state in the square and honeycomb lattices for $U/w = 3/2$, which is beyond the critical value for the formation of the Mott insulator in the latter, and for two values of T/w that are very close in both lattices. With decreasing temperature, n vs μ reveals the single-particle gap in the Mott phase by exhibiting a region in which n barely changes

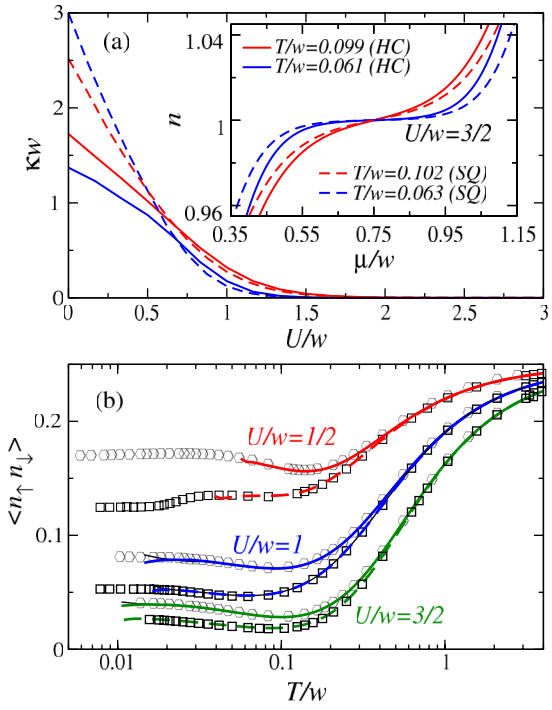

FIG. 1 (color online). (a) NLCE results for the compressibility vs U in the honeycomb (HC) and square (SQ) lattices, at half filling, for two values of T/w that are very close in both lattices. *Inset*- Equation of state for $U/w = 3/2$ and the same two values of T/w as in the main panel. These results were obtained after three cycles of improvement of Wynn's resummation algorithm [26]. The zero chemical potential, which corresponds to half filling for the particle-hole symmetric Hamiltonian, is shifted by $U/2$ for the nonsymmetric representation of the Hamiltonian in Eq. (1). (b) DQMC (symbols) and NLCE (lines) results for $\langle \hat{n}_\uparrow \hat{n}_\downarrow \rangle$ vs T in both lattices at half filling for $U/w = 1/2$, 1, and 3/2. Hexagons (Squares) and solid (dashed) lines correspond to honeycomb (square) lattice. Statistical error bars for DQMC data are shown only when they are greater than the symbol size. The NLCE results were obtained using Euler resummation, and we report the last order (thick lines) and the one to last order (black thin lines).

when changing μ. As expected from their phase diagrams, that gap is greater in the square lattice than in the honeycomb lattice. This results in the former system being less compressible than the latter at half filling and finite T for large values of U.

By decreasing T for small U, the compressibility ($\kappa = \partial n/\partial \mu$) also reveals the vanishing of the density of states in the semimetallic phase. This is shown in the main panel of Fig. 1(a), where, for weak interactions, the compressibility in the honeycomb lattice is seen to decrease with decreasing temperature ($\kappa \to 0$ as $T \to 0$). This behavior is to be contrasted with the one in the square lattice, where κ increases as $U \to 0$ and $T \to 0$, signaling the metal insulator transition [21]. Note that, for finite T, the behavior above leads to a region in U where κ is smaller in the honeycomb lattice than in the square lattice, despite the fact that in such a region the ground state in the former may be a semimetal while in the latter is an insulator. This can be understood given the difference between dispersion relations in the two systems which, at low T, can lead to less states being available in the honeycomb lattice than in the square lattice.

Another quantity of much interest, which can also be measured in experiments with ultracold fermions [32], is the double occupancy $\langle \hat{n}_\uparrow \hat{n}_\downarrow \rangle$. At half filling, $\langle \hat{n}_\uparrow \hat{n}_\downarrow \rangle$ is expected to decrease with decreasing temperature. This can be seen in Fig. 1(b), where we plot DQMC (symbols) and NLCE (lines) results for the double occupancy vs T for three values of U in the honeycomb and square lattices. (Note the excellent agreement between the results obtained utilizing the two approaches.) At high temperatures, $\langle \hat{n}_\uparrow \hat{n}_\downarrow \rangle$ is essentially the same for both geometries. However, as the double occupancy decreases when reducing T, one can see that the results in the honeycomb lattice depart from, and remain at higher values than, those in the square lattice. As this occurs, an upturn can be seen in the double occupancy with decreasing T. Especially for small U/w, this upturn is more pronounced in the honeycomb lattice than in the square lattice (note that for $U/w = 1/2$, it is absent in the latter geometry).

The existence of a region in temperature in which there is an anomalous $d\langle \hat{n}_\uparrow \hat{n}_\downarrow \rangle/dT < 0$ has been discussed in the context of the Hubbard model in the square lattice. Early dynamical mean-field theory calculations identified a significant anomalous region [33], which was later found to be marginal in DQMC [34] and NLCE [29] calculations in two dimensions (2D). Interest in the existence of such a region developed as it signals adiabatic cooling with increasing U. This follows from the relation $\partial S/\partial U = -\partial \langle \hat{n}_\uparrow \hat{n}_\downarrow \rangle/\partial T$ [33], which implies that at constant T, the entropy (S) increases (or, that at constant S, the temperature decreases) with increasing U. DQMC [34] and NLCE [29] calculations have also shown that, starting with short-range spin correlation for small values of U, one can generate exponentially large AF correlations by adiabatically increasing U, despite the fact that there is almost no

cooling for weak interactions. However, the entropy per particle needs to be $S \lesssim 0.5$.

We plot in Fig. 2, the isentropic curves in the T-U plane for the honeycomb lattice. By comparing those results with the ones for the square lattice (see Refs. [29,34] and the results for $S = 0.2$ in Fig. 2), it becomes apparent that adiabatic cooling is more significant in the honeycomb lattice for small values of U. This occurs in the absence of a Mott insulating ground state and where the available number of states at any given T in the honeycomb lattice is smaller than in the square lattice [see the compressibilities in Fig. 1(a)]. One may wonder if this could ease the realization of exponentially large AF correlations in the honeycomb lattice in comparison to the square lattice, where it remains a major experimental goal [35]. The region with exponentially large correlations can be identified from T^*, which is the temperature at which the uniform susceptibility is maximal for U beyond the critical value for the formation of the Mott insulator. T^* is also plotted in Fig. 2 and shows that an entropy per particle $S \lesssim 0.6$ is needed to generate exponentially large correlations in the honeycomb lattice. This is close to, but above, the entropy required in the square lattice. The entropy per particle at T^* in the square and honeycomb lattices for half filled systems, S^*, is shown in the inset of Fig. 2. Beyond $U/w = 1$, S^* can be seen to be almost the same in both lattice geometries ($S^* \lesssim 0.5$).

Probing long-range AF correlations turns out to be very challenging in optical lattice experiments. As a first step towards this goal, and towards identifying the AF Mott insulator in the Hubbard model on the square lattice, experiments have already measured NN spin correlations S^{zz}_{nn} [36,37]. They increase as the temperature is lowered and can be significant even before long-range order sets in the system. In Fig. 3, we plot S^{zz}_{nn} in the square and honeycomb lattices vs S for two different values of U/w, one below and one above the critical value for the formation of the Mott insulator in the honeycomb lattice. That figure shows that, unexpectedly, there is an extended region in entropies where $|S^{zz}_{nn}|$ are greater in the honeycomb lattice than in the square lattice, and that this happens even when the ground state in the former is a semimetal or a spin liquid while it is an AF Mott insulator in the latter. At very low entropies, we find that, ultimately, $|S^{zz}_{nn}|$ in the square lattice becomes greater than in the honeycomb lattice, but the entropy at which this occurs becomes smaller as U increases.

Our results imply that strong NN spin correlations can be more easily observed in experiments in the honeycomb lattice than in the square lattice. They also make evident that an enhancement of $|S^{zz}_{nn}|$ should not be taken as a signature of the Néel state, which does not exist in the honeycomb lattice for $U/w < 0.72$, where $|S^{zz}_{nn}|$ is greater than in the square lattice (for entropies per particle that are currently achievable experimentally). This is because such an enhancement can be a very local effect. We have also calculated next-nearest-neighbor correlations, S^{zz}_{nnn}, in both lattices (see the inset of Fig. 3) and found them to be always stronger in the square lattice than in the honeycomb lattice.

Cooling fermions in optical lattices to realize the Néel state is currently one of the main experimental challenges [35]. To that purpose, one can take advantage of the fact that the system is inhomogeneous [a term $\sum_{i\sigma} V r_i^2 \hat{n}_{i\sigma}$, where V is the strength of the trapping potential and r_i is the distance of each lattice site to the center of the trap, needs to be added to Eq. (1)] and that this implies that the entropy is unevenly distributed in the gas [35]. Based on that idea, two recent works, one on the square lattice [29] and the other on the cubic lattice [38], have shown that starting with a system

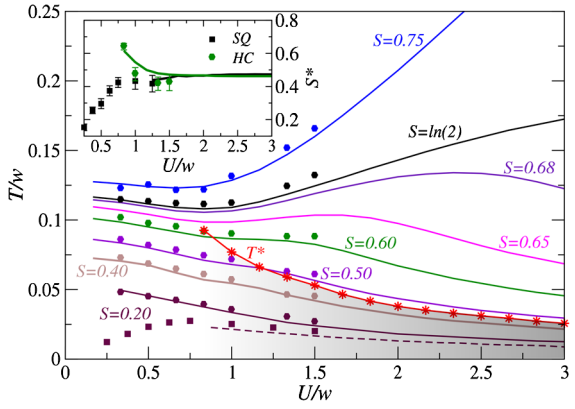

FIG. 2 (color online). Isentropic curves for the temperature vs U/w in the honeycomb lattice at half filling at several constant entropies. The crossover scale, T^*, from NLCE is only depicted in the regime where the ground state is a Mott insulator with long-range AF correlations. For $S = 0.20$, we also show results for the square lattice (dashed line and square symbols). The inset shows the entropy per particle at $T = T^*$ vs U/w. Lines (Symbols) correspond to NLCE (DQMC) results.

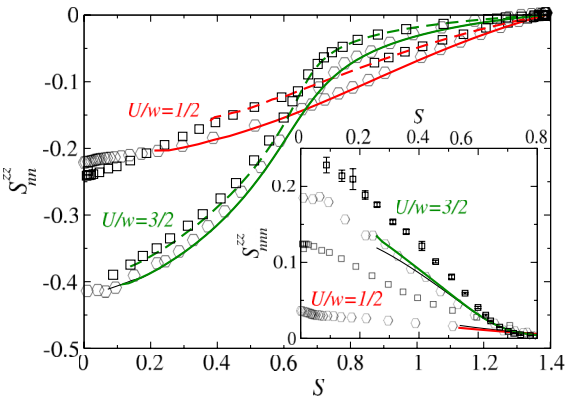

FIG. 3 (color online). (main panel) Nearest-neighbor spin correlations and (inset) next-nearest-neighbor spin correlations in the honeycomb and square lattices at half filling as a function of entropy, for $U = w/2$ and $3w/2$. Lines and symbols are the same as in Fig. 1(b). Note that, for S^{zz}_{nnn} in the square lattice, only DQMC results are shown.

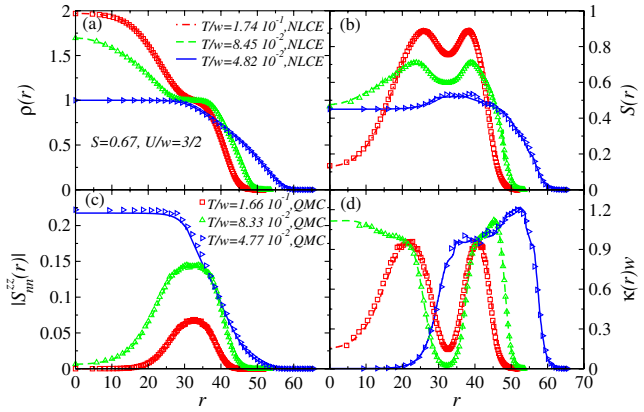

FIG. 4 (color online). (a) Density, (b) entropy, (c) NN spin correlations, and (d) compressibility for trapped honeycomb lattice systems with $N = 6.7 \times 10^3$ particles, an average entropy per particle $S = 0.67$, $U = 3w/2$, and $V/w = 1.5 \times 10^{-3}$, 1.0×10^{-3}, and 3.8×10^{-4} (in order of decreasing temperature). DQMC results are depicted as symbols and NLCE results as lines. Note that, due to the finite T grids used in DQMC and NLCE calculations, the values of T in both approaches are very close but not identical.

with high density in the center of the trap ($n \sim 2$) and with an average entropy per particle larger than S^*, one can achieve a Mott insulator in the center of the trap with a local entropy smaller than or equal to S^* by adiabatically decreasing the confining potential. The excess entropy is then stored in the compressible domains with $n < 1$.

In Fig. 4, we use the local density approximation, combined with DQMC and NLCE calculations of the homogeneous system, to show how the cooling mechanism discussed above works in the honeycomb lattice. (For temperatures like the ones studied here, DQMC calculations have shown that local density approximation is a good approximation on the square lattice [39].) Figure 4 depicts the evolution of the local density (a), local entropy (b), NN spin correlations (c), and the local compressibility (d) as one reduces the trapping potential adiabatically in a system with $U/w = 3/2$ and in which the average entropy per particle is $S = 0.67$. This entropy per particle is higher than $S^* = 0.47$ for $U/w = 3/2$. One can see that, as V is reduced, the density in the center of the trap changes from nearly that of a band insulator to that of a Mott insulator [Fig. 4(a)]. At the same time, the entropy in the Mott insulating region becomes of the order of, or smaller than, S^*, with the excess entropy being moved to the metallic wings [Fig. 4(b)]. This results in strong NN correlations in the Mott insulating domain [Fig. 4(c)] and a vanishing compressibility in the same region [Fig. 4(d)]. Our results for a specific trapping potential and number of particles (similar to the ones in current experiments) can be extended to other values of the trapping potential and number of particles through the use of the characteristic density [40,41].

In summary, we have used DQMC and NLCEs to study experimentally relevant thermodynamic properties and spin correlations of the Hubbard model in the honeycomb lattice. We find that, at half filling and weak interactions, the compressibility in this lattice may be smaller than in the square lattice at low T, despite the fact that the ground state in the former is a semimetal and in the latter an insulator. We also find that the honeycomb lattice exhibits a more significant anomalous region with $d\langle\hat{n}_\uparrow\hat{n}_\downarrow\rangle/dT < 0$ than the square lattice, which leads to a stronger adiabatic cooling in the former lattice geometry. Remarkably, NN spin correlations in the honeycomb lattice are stronger than in the square lattice in an extended region of entropies for all U. We discussed how these findings are reflected in optical lattice experiments.

This work was supported by NSF Grant No. OCI-0904597 (B. T., E. K., and M. R.), and by CNPq, FAPERJ, and INCT on Quantum Information (TP). T. P thanks R. T. Scalettar and L. G. Marcassa for discussions.

[1] K. S. Novoselov, A. K. Geim, S. V. Morozov, D. Jiang, Y. Zhang, S. V. Dubonos, I. V. Grigorieva, and A. A. Firsov, Science **306**, 666 (2004).
[2] A. H. Castro Neto, F. Guinea, N. M. R. Peres, K. S. Novoselov, and A. K. Geim, Rev. Mod. Phys. **81**, 109 (2009).
[3] Z. Y. Meng, T. C. Lang, S. Wessel, F. F. Assaad, and A. Muramatsu, Nature (London) **464**, 847 (2010).
[4] S. Sorella and E. Tosatti, Europhys. Lett. **19**, 699 (1992).
[5] T. Paiva, R. T. Scalettar, W. Zheng, R. R. P. Singh, and J. Oitmaa, Phys. Rev. B **72**, 085123 (2005).
[6] S. Sorella, Y. Otsuka, and S. Yunoki, arXiv:1207.1783v1.
[7] A. Mulder, R. Ganesh, L. Capriotti, and A. Paramekanti, Phys. Rev. B **81**, 214419 (2010).
[8] R. Ganesh, D. N. Sheng, Y.-J. Kim, and A. Paramekanti, Phys. Rev. B **83**, 144414 (2011).
[9] D. C. Cabra, C. A. Lamas, and H. D. Rosales, Phys. Rev. B **83**, 094506 (2011).
[10] H. Mosadeq, F. Shahbazi, and S. A. Jafari, J. Phys. Condens. Matter **23**, 226006 (2011).
[11] A. F. Albuquerque, D. Schwandt, B. Hetényi, S. Capponi, M. Mambrini, and A. M. Läuchli, Phys. Rev. B **84**, 024406 (2011).
[12] B. K. Clark, D. A. Abanin, and S. L. Sondhi, Phys. Rev. Lett. **107**, 087204 (2011).
[13] F. Mezzacapo and M. Boninsegni, Phys. Rev. B **85**, 060402(R) (2012).
[14] J. Reuther, D. A. Abanin, and R. Thomale, Phys. Rev. B **84**, 014417 (2011).
[15] W. Wu, S. Rachel, W.-M. Liu, and K. Le Hur, Phys. Rev. B **85**, 205102 (2012).
[16] M. Gibertini, A. Singha, V. Pellegrini, M. Polini, G. Vignale, A. Pinczuk, L. N. Pfeiffer, and K. W. West, Phys. Rev. B **79**, 241406(R) (2009).
[17] A. Singha, M. Gibertini, B. Karmakar, S. Yuan, M. Polini, G. Vignale, M. I. Katsnelson, A. Pinczuk, L. N. Pfeiffer, K. W. West, and V. Pellegrini, Science **332**, 1176 (2011).

[18] L. Tarruell, D. Greif, T. Uehlinger, G. Jotzu, and T. Esslinger, Nature (London) **483**, 302 (2012).
[19] K. K. Gomes, W. Mar, W. Ko, F. Guinea, and H. C. Manoharan, Nature (London) **483**, 306 (2012).
[20] I. Bloch, J. Dalibard, and W. Zwerger, Rev. Mod. Phys. **80**, 885 (2008).
[21] M. Imada, A. Fujimori, and Y. Tokura, Rev. Mod. Phys. **70**, 1039 (1998).
[22] D. J. Scalapino and R. L. Sugar, Phys. Rev. Lett. **46**, 519 (1981).
[23] E. Y. Loh and J. E. Gubernatis, in *Modern Problems in Condensed Matter Sciences*, edited by W. Hanke and Y. V. Kopaev (North-Holland, Amsterdam, 1992), Vol. 32, p. 177.
[24] A. Muramatsu, in *Quantum Monte Carlo Methods in Physics and Chemistry*, edited by M. P. Nightingale and C. J. Umrigar, NATO Science Series (Kluwer Academic Press, Dordrecht, 1999), p. 343.
[25] M. Rigol, T. Bryant, and R. R. P. Singh, Phys. Rev. Lett. **97**, 187202 (2006).
[26] M. Rigol, T. Bryant, and R. R. P. Singh, Phys. Rev. E **75**, 061118 (2007).
[27] M. Rigol, T. Bryant, and R. R. P. Singh, Phys. Rev. E **75**, 061119 (2007).
[28] B. Tang, E. Khatami, and M. Rigol, Comput. Phys. Commun. (in press).
[29] E. Khatami and M. Rigol, Phys. Rev. A **84**, 053611 (2011).
[30] W. S. Bakr, A. Peng, M. E. Tai, R. Ma, J. Simon, J. I. Gillen, S. Folling, L. Pollet, and M. Greiner, Science **329**, 547 (2010).
[31] J. F. Sherson, C. Weitenberg, M. Endres, M. Cheneau, I. Bloch, and S. Kuhr, Nature (London) **467**, 68 (2010).
[32] R. Jördens, N. Strohmaier, K. Günter, H. Moritz, and T. Esslinger, Nature (London) **455**, 204 (2008).
[33] F. Werner, O. Parcollet, A. Georges, and S. R. Hassan, Phys. Rev. Lett. **95**, 056401 (2005).
[34] T. Paiva, R. Scalettar, M. Randeria, and N. Trivedi, Phys. Rev. Lett. **104**, 066406 (2010).
[35] T. Esslinger, Annu. Rev. Condens. Matter Phys. **1**, 129 (2010).
[36] S. Trotzky, Y.-A. Chen, U. Schnorrberger, P. Cheinet, and I. Bloch, Phys. Rev. Lett. **105**, 265303 (2010).
[37] D. Greif, L. Tarruell, T. Uehlinger, R. Jördens, and T. Esslinger, Phys. Rev. Lett. **106**, 145302 (2011).
[38] T. Paiva, Y. L. Loh, M. Randeria, R. T. Scalettar, and N. Trivedi, Phys. Rev. Lett. **107**, 086401 (2011).
[39] S. Chiesa, C. N. Varney, M. Rigol, and R. T. Scalettar, Phys. Rev. Lett. **106**, 035301 (2011).
[40] M. Rigol, A. Muramatsu, G. G. Batrouni, and R. T. Scalettar, Phys. Rev. Lett. **91**, 130403 (2003).
[41] M. Rigol and A. Muramatsu, Opt. Commun. **243**, 33 (2004).